A METHOD FOR SELECTING VELOCITY FILTER CUTOFF FREQUENCY FOR MAXIMIZING IMPEDANCE WIDTH PERFORMANCE IN HAPTIC INTERFACES

Vinay Chawda
Department of Mechanical Engineering
and Materials Science
Rice University
Houston, TX 77005 USA
vinay.chawda@rice.edu

Ozkan Celik
School of Engineering
San Francisco State University
San Francisco, CA 94132 USA
ocelik@sfsu.edu

Marcia K. O'Malley *
Department of Mechanical Engineering
and Materials Science
Rice University
Houston, TX 77005 USA
omalleym@rice.edu

ABSTRACT

This paper analyzes the effect of velocity filtering cut-off frequency on the Z-width performance in haptic interfaces. Finite Difference Method (FDM) cascaded with a lowpass filter is the most commonly used technique for estimating velocity from position data in haptic interfaces. So far, there is no prescribed method for obtaining the FDM+filter cut-off frequency that will maximize the Z-width performance. We present a simulation based method to demonstrate that there exists such an ideal FDM+filter cut-off frequency, and that it can be predicted by numerical simulation. Experiments are conducted on a single degree-of-freedom linear haptic interface to validate the simulation results.

1 Introduction

Impedance width, or Z-width, is the dynamic range of impedances that can be passively rendered by a haptic interface. Z-width was proposed by Colgate and Brown [1] as a fundamental measure of performance for haptic interfaces. A larger achievable dynamic range of impedances translates to a more realistic haptic rendering of a virtual environment. Therefore, it is desirable to maximize the Z-width boundary of a haptic display. The Z-width boundary is dependent upon various parameters of the haptic interface such as the device dynamics [2], sampling frequency [3], position sensor quantization [4], [5], [1], actuator saturation [6], time delays [7] and velocity estimation [8], [9]. In this study, we investigate the effect of velocity filter cut-off frequency on the Z-width performance. Specifically, we conduct numerical simulations that are supported by experiments to demonstrate that there is an ideal velocity filter cut-off frequency which maximizes the Z-width performance of a haptic interface, and its value can be predicted by simulation.

In haptic applications, velocity is typically estimated from the position encoder data using the finite difference method (FDM), or equivalently the backward difference method for real time implementation. The velocity obtained by FDM is very noisy due to sampling and quantization effects, and a low pass filter is required to smooth the signal [1]. Choice of the FDM+filter cut-off frequency determines the phase distortion introduced in the velocity signal, and the amount of noise present after filtering. At lower cut-off frequencies, the phase distortion is high and the noise permitted through is minimal. Conversely, as the cut-off frequency increases the phase distortion of the velocity signal decreases, but at the cost of allowing more noise to pass through the filter. This trade-off between time-delay and noise in velocity signals suggests that there is a dependance of Z-width performance on the FDM+filter cut-off frequency, since the accuracy of velocity estimation directly affects the Z-width performance [8].

Researchers have proposed advanced velocity estimators to overcome the trade-off between time-delay and accuracy in velocity estimates, such as Kalman filters [10], Taylor's series expansion and least-square fit estimators [11], first-order adaptive windowing [9], Levant's differentiator [8], time-stamping [12], [13], position and acceleration based velocity estimation [14], and Luenberger and other nonlinear velocity observers [15], [16], [17], [18], [19], [20]. However, these advanced velocity estimation techniques suffer from constraints such as higher computation time, special hardware requirements, parameter tuning; and on many occasions, the implementation is tedious or not possi-

*Address all correspondence to this author.

ble within the framework of existing control hardware. For these reasons, FDM+filter is still the most commonly used method for velocity estimation. Despite its ubiquitous use for velocity estimation, few researchers have specifically addressed the effect of FDM+filter cut-off frequency selection on Z-width performance.

In many haptic applications, the cut-off frequency in the FDM+filter velocity estimation method is either chosen in an ad-hoc fashion [1], [21] or is manually tuned for a given application [22]. Several researchers have used FDM+filter as a benchmark in comparing advanced velocity estimation methods, but the FDM+filter cut-off frequency was chosen in an ad-hoc fashion [9], [23], [24], [14]. Diaz et al. proposed that FDM+filter cut-off frequency be chosen in range between the bandwidth of the human hand (∼10 Hz, [25]) and the first vibration mode of the haptic interface device [7]. This method still leaves a lot of room for the selection of the cut-off frequency, which is commonly chosen near the allowable lower bound in the literature.

In this paper, we studied the effect of FDM+filter cut-off frequency on Z-width performance of a haptic display by conducting linear stability analysis, numerical simulations and experimental analysis. We found that there is an "ideal" cut-off frequency which maximizes the Z-width performance of a haptic device, and its value can be predicted by numerical simulation. The simulation is conducted using a linear device model obtained by performing system identification of the haptic device, and considering the actuator saturation and position quantization nonlinearities. The ideal FDM+filter cut-off frequency and the variation of Z-width performance with varying cut-off frequencies predicted by the simulation is validated experimentally. It is found that the linear stability analysis is not sufficient to predict the ideal FDM+filter cut-off frequency, as position sensor quantization plays an important role in determination of the ideal cut-off frequency. We show that numerical simulation considering the quantization nonlinearity provides an effective way of identifying the FDM+filter cut-off frequency that will maximize the Z-width performance in a haptic device.

The paper is organized as follows. In Section 2, we present a linear stability analysis-based approach, a numerical simulation-based approach and finally experimental analysis, for exploring the effect of FDM+filter cut-off frequency on the Z-width performance. In Section 3, we discuss the results from the linear analysis, simulations and experiments, and comment on the contributions of this study. Finally, we conclude the paper in Section 4.

2 Methods to explore effect of velocity filter cut-off frequency on Z-width performance

2.1 Linear Analysis

Linear stability analysis of a single degree of freedom linear impedance type haptic interface device is employed to study the effect of velocity lowpass filter cut-off frequency on the Z-width of haptic devices. The analysis is based on the approach proposed by Gil et al. in [26]. Consider a single-DOF haptic interface schematic as shown in Fig. 1 with a mass-spring-damper model ($G(s)$) for the haptic device and velocity estimated using FDM+second order Butterworth lowpass filter. With an aim to minimize delay in estimations, we limit ourselves to a second order filter. The continuous time transfer function of a second order lowpass Butterworth filter is given as

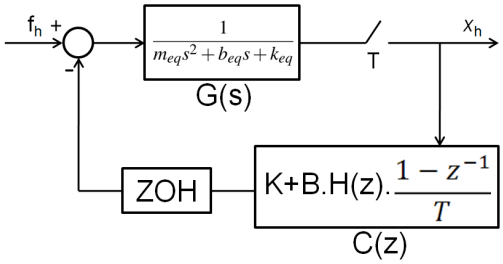

Figure 1. Block diagram showing the single-DOF haptic interface with velocity estimated using FDM+filter. $G(s)$ represents the haptic device, $C(z)$ represents the virtual environment and f_h is the force applied by the human.

$$G(s) = \frac{G_0\omega_c^2}{s^2 + 1.414s\omega_c + \omega_c^2} \tag{1}$$

where G_0 is the DC gain and ω_c is the cutoff frequency. We used the bilinear transform to obtain the discrete time transfer function ($H(z)$) of the lowpass second order Butterworth filter with sampling period T, given as:

$$\begin{aligned} H(z) &= \frac{N(z)}{D(z)}, \text{ where} \\ N(z) &= G_0T^2(z+1)^2\omega_c^2 \quad \text{and} \\ D(z) &= (4+2.8\omega_cT+T^2\omega_c^2)z^2 + (2T^2\omega_c^2-8)z \\ &\quad +(4+T^2\omega_c^2-2.8\omega_cT) \end{aligned} \tag{2}$$

Bilinear transformation is used because it preserves the causal, stable nature of the continuous time system while mapping to the discrete domain.

The virtual environment is modeled as a spring-damper virtual wall ($C(z)$) with virtual wall stiffness (K) and virtual wall damping (B). The force applied by the human operator is f_h, and x_h is the position output of the haptic device.

The discrete time closed loop transfer function of the system shown in Fig. 1 is given by:

$$x_h = \frac{Z[Gf_h]}{1+Z[ZOH\ G]C(z)} \tag{3}$$

where Z is the Z-transform operator and ZOH is the zero-order-hold. The characteristic equation is given as

$$1+Z[ZOH\ G]C(z) = 0. \tag{4}$$

The characteristic equation can be used to find the stability boundary.

$$1+Z[ZOH\ G]\left(K+BH(z)\frac{1-z^{-1}}{T}\right)=0$$

$$\text{or, } 1+K\left(\frac{Z[ZOH\ G]}{1+Z[ZOH\ G]BH(z)\frac{1-z^{-1}}{T}}\right)=0$$

The stability region is determined by the (K,B) pairs which satisfy the inequality

$$K<GM\left(\frac{Z[ZOH\ G]}{1+Z[ZOH\ G]BH(z)\frac{1-z^{-1}}{T}}\right) \tag{5}$$

where $GM(.)$ is the gain margin.

The device parameters were specified as m_{eq} = 0.4160 kg, b_{eq} = 5.5195 N.s/m and k_{eq} = 11.0626 N/m. For a particular cut-off frequency ω_c, virtual wall damping B is varied and the corresponding values of K satisfying the inequality (5) constitute the 'uncoupled stability' boundary. Uncoupled stability does not consider the coupling of human operator with the haptic device, resulting a larger region of stability encompassing the Z-width [27]. The plot of maximum values of K satisfying the inequality (5) for varying B gives the uncoupled stability boundary. The approach followed in conducting the linear analysis assumes that for chosen device parameter values, gain margin is well defined for the range of ω_c and B considered. If these parameters are allowed to take any arbitrary value, then it is possible to have multiple crossings of phase at negative 180 degrees and gain margin will not be well defined. In that case above approach is not applicable.

Figure 2 shows the uncoupled stability boundary plots obtained by the linear analysis for varying cut-off frequencies. It is observed that with increasing cut-off frequencies, the boundary increases. It should be noted that the Z-width boundary will always be smaller than the uncoupled stability boundary, and in practice will be further limited due to actuator saturation, quantization, friction and other nonlinearities.

2.2 Simulation analysis considering nonlinearities

The linear analysis in the previous section did not take into account some important nonlinearities such as actuator saturation and quantization. Actuator selection depends on the target application and design requirements of the haptic device, and will dictate the actuator saturation limits. Position sensor quantization on the other hand, is something that can be selected independently of the hardware design requirements, and is very important for the accuracy of the haptic device control. Position sensor quantization directly affects the velocity estimation, and consequently the Z-width performance. We performed system identification of a single degree of freedom (DOF) haptic interface device, and used the identified model in the simulation for estimating the Z-width boundaries, and studied the effect of velocity filter cut-off frequency on Z-width performance. We will first briefly describe the single-DOF haptic interface device and the system identification for identifying the model parameters, and then present the simulation methodology to estimate the Z-width boundary.

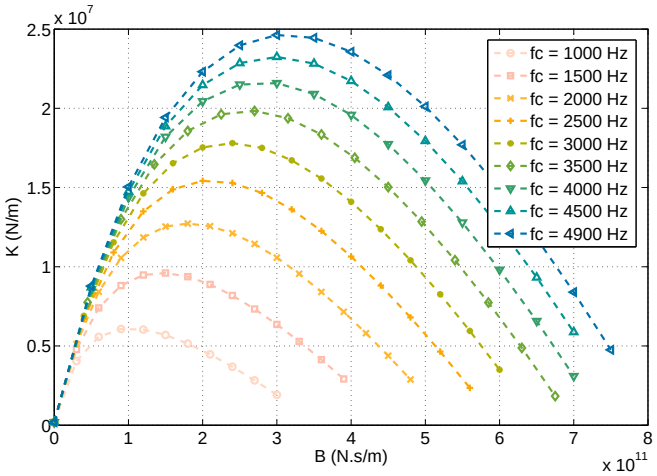

Figure 2. Z-width plots are obtained analytically for a single-DOF haptic device with velocity estimated using FDM+filter. The sampling frequency is fixed at 10kHz and the plots are generated for varying cut-off frequencies ($f_c = \omega_c/2\pi$)

2.2.1 Single degree of freedom haptic interface

The Z-width experiments were performed on a custom built single degree-of-freedom, linear, impedance type haptic interface device. The device is shown in Fig. 3. The haptic interface has a workspace of 0.15 m and the handle position is measured by a linear incremental encoder with a resolution of 1 μm. A detailed description and technical specifications of the device can be found in [8].

2.2.2 System identification and simulation model

A physics-based model of the single-DOF haptic interface device was developed, given as

$$m_{eq}\ddot{x}+b_{eq}\dot{x}+k_{eq}(x-x_0)=k_{DAQ}V_{in} \tag{6}$$

where x is the handle position, m_{eq} is the equivalent mass of the system comprising of the cart mass and motor inertia, b_{eq} is equivalent physical damping in the system, k_{eq} is the equivalent stiffness of the system arising from the capstan drive dynamics [28], and x_0 is the equilibrium position for this equivalent spring. k_{DAQ} is the gain relating the voltage input to the force output of the motor+capstan drive. Gray-box system identification was performed in the time domain to identify the parameter

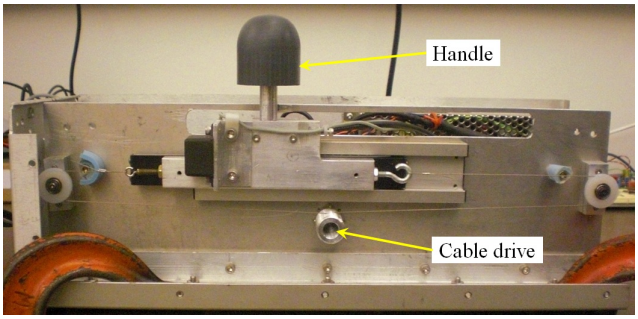

(a) Front view

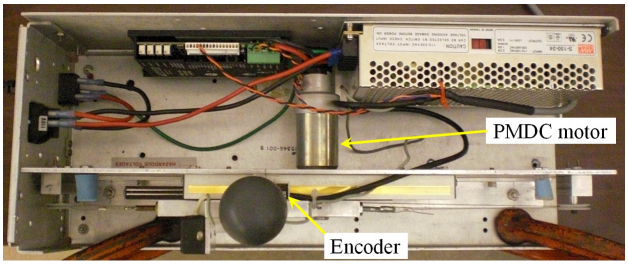

(b) Top view

Figure 3. A single degree-of-freedom haptic device is used as the experimental setup.

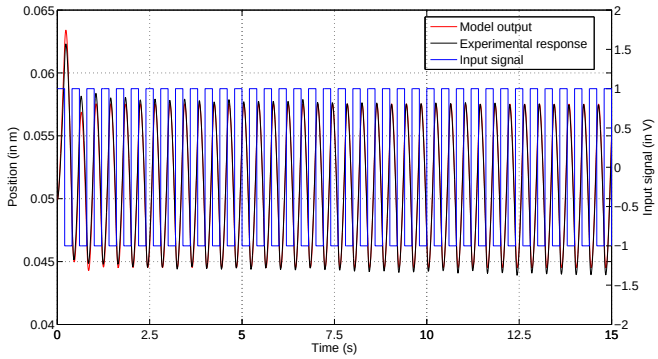

Figure 4. Time response of the identified model and experimental response for a pulse voltage input signal. The gradual shift in mean position of the response plots is due to the spring term $k_{eq}(x - x_0)$.

values. k_{DAQ} was estimated as $k_{DAQ} = k_t k_{amp}/r_c$, where k_t is the torque constant of the motor, k_{amp} is the voltage-to-current amplifier gain and r_c is the radius of the capstan drum. The average parameter values were identified as $m_{eq} = 0.4160kg$, $b_{eq} = 5.5195N.s/m$, $k_{eq} = 11.0626N/m$, $x_0 = 0.0517m$ and $k_{DAQ} = 0.5906N/V$. Figure 4 shows the time response of the identified model and experimental response for a pulse input signal.

The schematic of the simulation model is shown in Fig. 5. The single-DOF haptic interface device was modeled as (6). A hybrid simulation model was constructed using a continuous solver to simulate the single-DOF device and a fixed step solver to simulate the discrete time control. The virtual wall was simulated at 10kHz and the actuation rate was fixed at 1kHz. The actuation rate is chosen smaller than the control loop rate because in the experimental setup we are using a Pulse Width Modulation (PWM) amplifier with a switching frequency of 36kHz, and for an actuation rate of 10kHz, the PWM amplifier is unlikely to run the current control loop sufficiently fast. The saturation limits imposed by the data acquisition card are +/-10V. MATLAB® and SIMULINK® were used to perform the simulation.

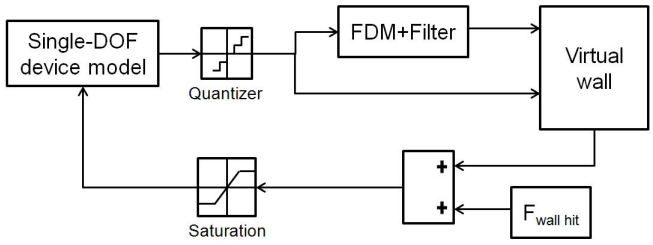

Figure 5. Schematic showing the simulation of the single-DOF haptic interface device with velocity estimated using FDM+filter.

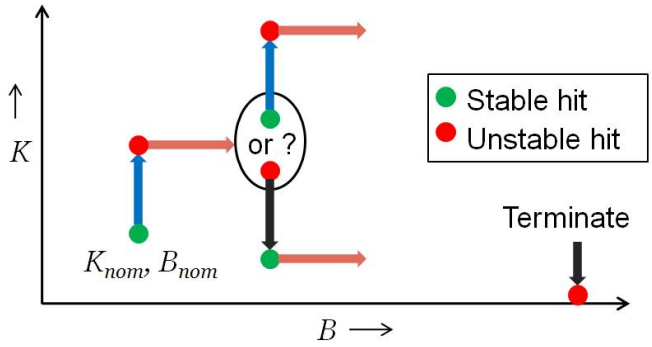

Figure 6. Schematic showing the automated wall hit task protocol adopted in simulation and experiments for estimating the Z-width boundary in the single-DOF haptic interface device.

2.2.3 Automated wall-hit protocol for estimating Z-width We simulated the experimental protocol adopted in our previous work [8] to estimate the Z-width boundary. At the beginning of the experiment, the handle was placed 0.07m away from the virtual wall. A constant torque was commanded to the motor resulting in an effective force of 2.835 N at the handle, driving it towards the wall. After allowing a 4 second period for the wall hit to reach steady state, mean position was recorded. Root Mean Square (RMS) difference between the mean position and the instantaneous position of the handle was computed for the next 2 seconds, and if this RMS difference was smaller than a threshold ε, then there were no sustained oscillations present at the steady state. A wall hit was declared stable if there were no sustained oscillations at the steady state. We chose $\varepsilon = 1.5 \times 10^{-5}m$ for our experiments. Although the specific value of ε affects the size of the Z-width boundary, it does not affect the qualitative dependance of the Z-width performance on the velocity cut-off frequency. We started with a nominal

value of virtual wall stiffness (K) and virtual wall damping (B) for which the wall hit was stable. K was increased in steps until an unstable wall hit was observed, at which point B was incremented by a step. If the wall hit was stable after incrementing B, then K was incremented until an unstable wall hit was observed, else K was decremented until a stable wall hit was observed. B was again incremented and the whole cycle repeated until the virtual wall was not stable for any value of K. The plot of K vs. B for which the virtual wall was marginally stable constitutes the Z-width boundary. This automated wall hit task protocol is schematically shown in Fig. 6.

Figure 7 shows the Z-width plots obtained by simulation. It is observed in Fig. 7(a) that for a position quantization of $1\mu m$, the Z-width performance saturates after initially increasing monotonically with increasing cut-off frequency until around $f_c = 2000Hz$. No significant increase in Z-width performance is observed after $f_c = 2000Hz$. On doubling the position quantization to $2\mu m$, the saturating trend observed earlier changes and the Z-width performance begins to decrease after reaching a peak at $f_c = 1700Hz$, as shown in Fig. 7(b).

2.3 Experimental Analysis

Experiments were conducted on the single-DOF device to observe the effect of changing velocity filter cut-off frequency on the Z-width performance, and validate the predictions of the simulation analysis. The automated wall hit task protocol described in the previous section was used to obtain the experimental Z-width plots. The control was implemented using SIMULINK and QUARC toolbox on a host PC running Windows XP. The code was compiled and downloaded on a target computer running QNX real time operating system. The target computer interfaced with the single-DOF haptic interface device through a Q4 data acquisition card from Quanser Inc. The sampling frequency was fixed at 10kHz and the actuation rate was set at 1kHz. This allows the velocity estimation and filtering to run at 10kHz, while actuating at a lower rate to avoid the confounding effects of PWM amplifier switching frequency. The virtual wall is effectively rendered at 1kHz, but with improved velocity estimation due to higher sampling rate. The Z-width boundaries are plotted for velocity filtered with varying cut-off frequencies. Figure 8(a) and (b) show the plots with $1\mu m$ and $2\mu m$ position quantization. The position encoder on the device has a position quantization of $1\mu m$, and for obtaining the plots in Fig. 8(b) the quantization was artificially increased in software.

3 Discussion

Impedance width in a single degree of freedom haptic interface device is analyzed using three techniques: linear stability analysis, numerical simulation considering the position sensor quantization and actuator saturation nonlinearities, and experimental methods. The goal of these analyses is to observe the effect of velocity filter cut-off frequency on Z-width performance, and investigate if there is an "ideal" cut-off frequency that maximizes the Z-width performance.

Figure 2 shows the variation of uncoupled stability boundary plots obtained with linear analysis. It is observed that with increasing cut-off frequencies, the uncoupled stability boundary increases monotonically, which suggests that the Z-width boundary plots might also follow the same trend. The magnitude of the uncoupled stability boundary only gives a theoretical envelope of the Z-width boundary magnitude. The plots obtained with linear analysis do not consider any quantization in position sensing or actuator saturation. To make reasonable predictions about the effect of FDM+filter cut-off frequency on the Z-width performance, a more realistic model of the physical system considering the nonlinearities like position quantization and actuator saturation is needed. A hybrid model incorporating the continuous device dynamics and the discrete sampled and quantized feedback controller would capture the aforementioned nonlinearities, but will not lend itself to easily to analytical stability analysis. Hence, we performed system identification to estimate the physical system parameters, and a numerical simulation incorporating the position quantization and actuator saturation to estimate Z-width performance. The Z-width plots obtained by the simulation are shown in Figure 7. The simulation plots differ from the plots obtained by linear analysis on several points. Firstly, the magnitudes of the simulation plots are orders of magnitude lower than those obtained by linear analysis. This is expected due to actuator saturation and position quantization effects, which degrade the Z-width performance severely from the ideal case. Secondly, as observed in Figure 7(a), the Z-width plots increase in size with increasing FDM+filter cut-off frequency until $f_c = 2000Hz$, and beyond that no significant increase in Z-width performance is observed. This saturation in Z-width performance was not observed with linear analysis as seen in Fig. 2.

Position quantization directly affects the velocity estimation, as any quantization means loss of position information. An increase in quantization will mean that position is held constant for a longer period of time, causing drastic jumps in velocity estimation by FDM. Filtering will smooth down these jumps, and level of smoothing will depend on the choice of cut-off frequency. A higher quantization will require more smoothing, implying use of lower filter cut-off frequencies, which leads to higher phase distortion and degradation of Z-width performance. This hypothesis is validated by comparing the plots in Fig. 7(a) with $1\mu m$ quantization, with plots in Fig. 7(b) with $2\mu m$ quantization. It is observed that with increase in quantization, the saturating trend in Z-width performance observed in Fig. 7(a) changes and we observe a peak Z-width performance at $f_c = 1700Hz$, after which the Z-width performance starts falling down. The Z-width performance is lower at low cut-off frequencies due to the phase distortion introduced by excessive smoothing by the filter, and degradation of Z-width performance at higher cut-off frequencies is due to passing through of the chatter in velocity signal introduced by the increased quantization. At lower quantization, once the cut-off frequency reached the point where phase distor-

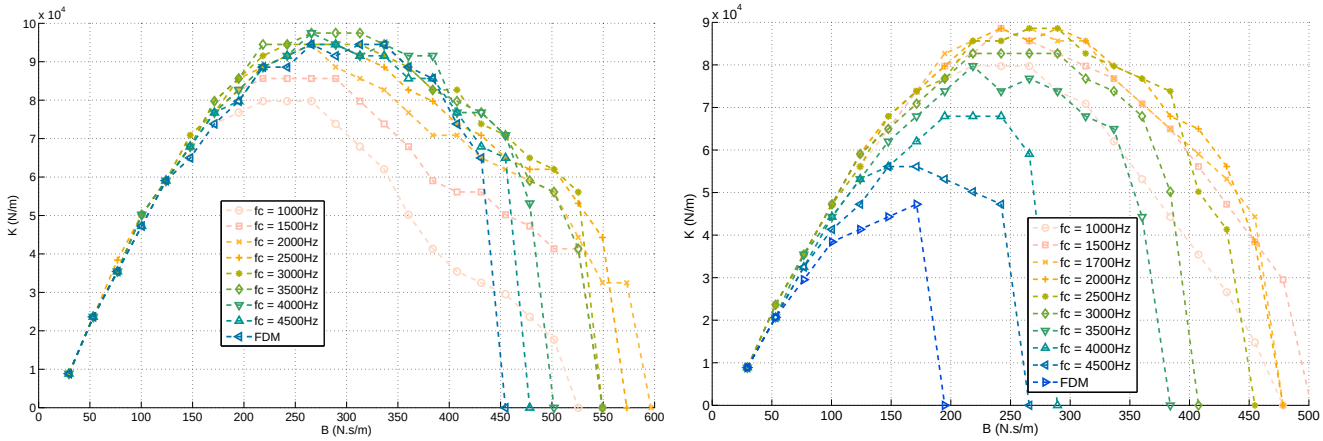

(a) Position quantization = $1\mu m$ (b) Position quantization = $2\mu m$

Figure 7. Z-width boundary plots obtained by simulation of the single-DOF haptic interface device with velocity estimated using FDM+filter. The sampling frequency was kept fixed at 10kHz and the plots were obtained for varying filter cut-off frequencies (f_c).

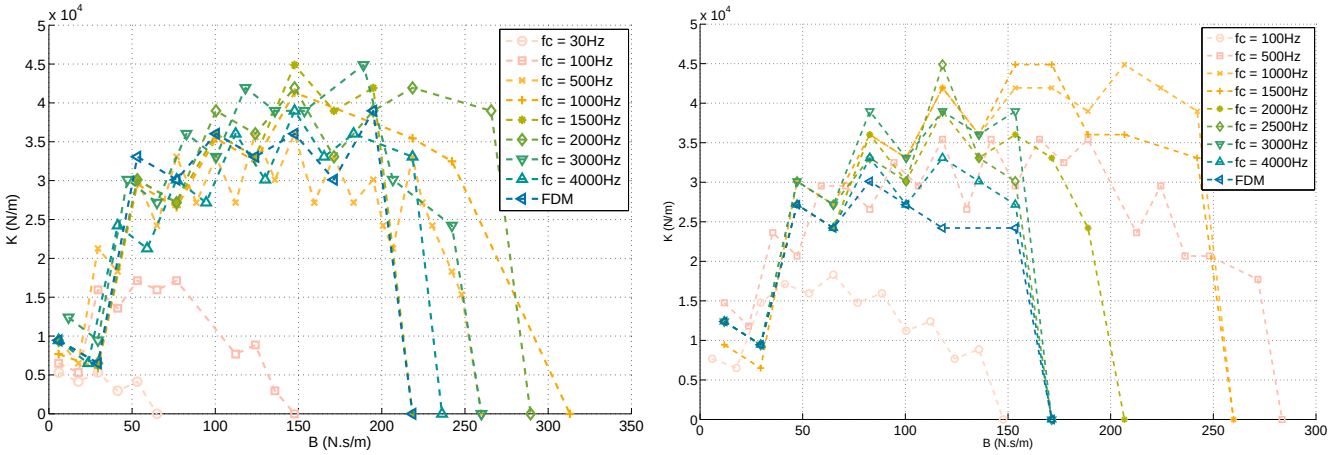

(a) Position quantization = $1\mu m$ (b) Position quantization = $2\mu m$

Figure 8. Experimentally obtained Z-width boundary plots from the single-DOF haptic interface device with velocity estimated using FDM+filter. The sampling frequency was kept fixed at 10kHz and the plots were obtained for varying filter cut-off frequencies (f_c).

tion by filter smoothing stopped being dominant, the chatter in velocity signal due to quantization was not large enough to cause any significant decrease in Z-width performance with increasing cut-off frequencies.

The experimental results are shown in Fig. 8, which validate the predictions from the simulation results shown in Fig. 7. It is observed in Fig. 8(a) that for a position quantization of $1\mu m$, the Z-width performance increases with increasing filter cut-off frequencies until saturating at $f_c = 2000Hz$, as predicted by the simulations in Fig. 7(a). Fig. 8(b) shows the Z-width plots when position quantization was set to $2\mu m$. The Z-width performance first increases, and then decreases with increasing filter cut-off frequencies, peaking at $f_c = 1500Hz$. The experimentally observed peak Z-width performance is close the value predicted by the simulation results, which is around $f_c = 1700Hz$ as shown in Fig. 7(b).

This study reports successful results in predicting an ideal FDM+filter cut-off frequency that maximizes the Z-width performance of the haptic interface device. Agreement between the experimental and simulated Z-width plots demonstrate that with a reasonably accurate model of the haptic interface, and accounting for quantization and actuator saturation, such an ideal cut-off frequency can be estimated via numerical simulation.

4 Conclusion

In this paper, we presented simulation and experimental results to show that there exists an ideal velocity filter cut-off frequency for maximizing the impedance width performance in haptic interfaces. We demonstrated that this ideal cut-off frequency can be predicted by conducting numerical simulations that use a reasonably accurate model of the haptic device and

consider the position quantization and actuator saturation nonlinearities. Furthermore, the value of the ideal cut-off frequency depends on the position sensor quantization, and with increase in quantization the ideal filter cut-off frequency and the maximum achievable Z-width performance decrease. It is also shown that the linear stability analysis is not sufficient to predict the effect of velocity filter cut-off frequency on Z-width performance.

ACKNOWLEDGMENT

This work was supported in part by NSF Grant CNS-1136099.

REFERENCES

[1] J. E. Colgate and J. M. Brown. Factors affecting the Z-width of a haptic display. In *International Conference on Robotics and Automation*, pages 3205–3210. IEEE, 1994.

[2] I. Díaz and J.J. Gil. Influence of vibration modes and human operator on the stability of haptic rendering. *IEEE Transactions on Robotics*, 26(1):160–165, 2010.

[3] M. K. O'Malley, K. S. Sevcik, and E. Kopp. Improved haptic fidelity via reduced sampling period with an FPGA-based real-time hardware platform. *Journal of Computing and Information Science in Engineering*, 9(1):011002–1–7, 2009.

[4] J.J. Abbott and A.M. Okamura. Effects of position quantization and sampling rate on virtual-wall passivity. *IEEE Transactions on Robotics*, 21(5):952–964, 2005.

[5] N. Diolaiti, G. Niemeyer, F. Barbagli, J.K. Salisbury, and C. Melchiorri. The effect of quantization and coulomb friction on the stability of haptic rendering. In *Symposium on Haptic Interfaces for Virtual Environment and Teleoperator Systems*, pages 237–246. IEEE, 2005.

[6] L.J. Tognetti. *Improved design and performance of haptic two-port networks through force feedback and passive actuators*. PhD thesis, Georgia Institute of Technology, 2005.

[7] I. Díaz, J.J. Gil, and T. Hulin. Chapter 5: Stability boundary and transparency for haptic rendering. *Advances in Haptics*, pages 103–125, April 2010.

[8] V. Chawda, O. Celik, and M. K. O'Malley. Application of Levant's differentiator for velocity estimation and increased Z-width in haptic interfaces. In *Proceedings of the IEEE World Haptics Conference 2011*, pages 403–408, Istanbul, Turkey, 2011.

[9] F. Janabi-Sharifi, V. Hayward, and C. S. J. Chen. Discrete-time adaptive windowing for velocity estimation. *IEEE Transactions on Control Systems Technology*, 8(6):1003–1009, 2002.

[10] P. R. Bélanger, P. Dobrovolny, A. Helmy, and X. Zhang. Estimation of angular velocity and acceleration from shaft-encoder measurements. *The International Journal of Robotics Research*, 17(11):1225–1233, 1998.

[11] R.H. Brown and S.C. Schneider. Velocity observations from discrete position encoders. In *International Conference on Industrial Electronics, Control, and Instrumentation*, pages 1111–1301, November 1987.

[12] P. Bhatti and B. Hannaford. Single-chip velocity measurement system for incremental optical encoders. *IEEE Transactions on Control Systems Technology*, 5(6):654 – 661, November 1997.

[13] RJE Merry, MJG Van de Molengraft, and M. Steinbuch. Velocity and acceleration estimation for optical incremental encoders. *Mechatronics*, 20(1):20–26, 2010.

[14] Wen-Hong Zhu and T. Lamarche. Damping enhancement of haptic devices by using velocities from accelerometers and encoders. In *Proceedings of the 48th IEEE Conference on Decision and Control, held jointly with the 28th Chinese Control Conference*, pages 7515 –7520, December 2009.

[15] R.D. Lorenz and K. Van Patten. High resolution velocity estimation for all digital, AC servo drives. In *Conference Record of the IEEE Industry Applications Society Annual Meeting*, volume 1, pages 363 –368, October 1988.

[16] Feng-Chieh Lin and Sheng-Ming Yang. Adaptive fuzzy logic-based velocity observer for servo motor drives. *Mechatronics*, 13(3):229 – 241, 2003.

[17] E.A. Baran, E. Golubovic, and A. Sabanovic. A new functional observer to estimate velocity, acceleration and disturbance for motion control systems. In *IEEE International Symposium on Industrial Electronics*, pages 384 –389, July 2010.

[18] L.K. Vasiljevic and H.K. Khalil. Differentiation with high-gain observers the presence of measurement noise. In *45th IEEE Conference on Decision and Control*, pages 4717–4722, 2006.

[19] A. Tilli and M. Montanari. A low-noise estimator of angular speed and acceleration from shaft encoder measurements. *Automatika*, 42(3-4):169–176, 2001.

[20] T. Nomura, Y. Kitsuka, and T. Matsuo. Non-model-based estimation for velocity and acceleration by adaptive identification method. *IEEJ Transactions on Electrical and Electronic Engineering*, 5(3):372–374, 2010.

[21] D.W. Weir, J.E. Colgate, and M.A. Peshkin. Measuring and increasing Z-width with active electrical damping. In *Haptic interfaces for virtual environment and teleoperator systems*, pages 169–175. IEEE, 2008.

[22] G. Liu. On velocity estimation using position measurements. In *Proceedings of the American Control Conference.*, volume 2, pages 1115–1120. IEEE, 2002.

[23] A. Levant. Robust exact differentiation via sliding mode technique. *Automatica*, 34(3):379–384, 1998.

[24] J.C. Metzger, O. Lambercy, and R. Gassert. High-fidelity rendering of virtual objects with the rehapticknob-novel avenues in robot-assisted rehabilitation of hand function. In *IEEE Haptics Symposium*, pages 51–56. IEEE, 2012.

[25] D.A. Lawrence, L.Y. Pao, M.A. Salada, and A.M. Dougherty. Quantitative experimental analysis of transparency and stability in haptic interfaces. In *Proc. Fifth*

Annual Symposium on Haptic Interfaces for Virtual Environment and Teleoperator Systems, pages 441–449, Nov. 1996.

[26] J.J. Gil, A. Avello, A. Rubio, and J. Florez. Stability analysis of a 1-DOF haptic interface using the Routh-Hurwitz criterion. *IEEE Transactions on Control Systems Technology*, 12(4):583 – 588, July 2004.

[27] J.E. Colgate and G. Schenkel. Passivity of a class of sampled-data systems: application to haptic interfaces. In *American Control Conference, 1994*, volume 3, pages 3236–3240, 1994.

[28] J. Werkmeister and A. Slocum. Theoretical and experimental determination of capstan drive stiffness. *Precision Engineering*, 31(1):55–67, 2007.